

POWER QUALITY IMPROVEMENT CONSIDERING VOLTAGE SAG AND UNBALANCE USING DVR

El-Zahraa. M. Mattar^{1*}, Ekramy. S Mahmoud¹, Mohamed. I. El-Sayed²

¹ Pyramids Higher Institute for Engineering and Technology, Cairo, Egypt

² Professor at Al-Azhar University, Faculty of Engineering, Cairo, Egypt

*Correspondence: elzahraamattar24@gmail.com,

Received: 31 Oct. 2022 Accepted: 17 Dec. 2022

ABSTRACT

According to recent power quality (PQ) studies, voltage sags and voltage unbalance in medium voltage and low voltage distribution grids are the most common type of power quality problems. This paper presents a solution to two different types of power quality issues; voltage sag and voltage unbalance. In order to study the actual impact of these two PQ issues, a study case based on real nonlinear loads data consists of large induction motors, located at Beshai Company in Sadat city, are investigate, the dynamic voltage restorer (DVR) is proposed to eliminate the voltage unbalance and the voltage sag problems. The dynamic voltage restorer is linked to the PCC to improve the PQ issues that have been identified. Matlab Simulink platform is used to simulate the power network, loads, and the dynamic voltage restorer (DVR). The jellyfish search optimizer (JFS) is utilized to get the gain values of the PI controller for the proposed DVR. The results of Matlab/Simulink advocate the proposed device's effectiveness, robustness, and latency.

KEYWORDS: Power quality problems, Voltage sag, Voltage unbalance, Dynamic voltage restorer.

تحسين جودة القدرة الكهربائية مع الأخذ في الاعتبار انخفاض الجهد وعدم اتزان الجهد باستخدام مسترجع الجهد الديناميكي

الزهراء محمود محمد^{1*}، اكرامى سعد محمود¹، محمد ابراهيم السيد²

¹ قسم هندسة القوى الكهربائية والتحكم، معهد الأهرامات العالي للهندسة والتكنولوجيا، القاهرة، مصر

² قسم هندسة القوى والآلات الكهربائية، كلية الهندسة، جامعة الأزهر، القاهرة، مصر

البريد الإلكتروني: elzahraamattar24@gmail.com

المخلص

وفقاً لدراسات جودة الطاقة الحديثة (PQ)، فإن انخفاض الجهد وعدم توازن الجهد في شبكات توزيع الجهد المتوسط والجهد المنخفض هي أكثر أنواع مشاكل جودة الطاقة شيوعاً. تقدم هذه الورقة حلاً لنوعين مختلفين من مشكلات جودة الطاقة؛ ترهل الجهد وعدم اتزان الجهد. تتم دراسة هاتين المسألتين PQ على أحمال حقيقية. توجد الأحمال غير الخطية من المحركات

الحنثية الكبيرة في شركة بشاي بمدينة السادات ، مصر. نظرًا لتأثير مشكلات PQ هذه عند نقطة توصيل مشتركة (PCC) ، يُقترح مسترجع الجهد الديناميكي (DVR) للتخفيف من هذه التأثيرات. يرتبط مسترجع الجهد الديناميكي بـ PCC لتحسين مشكلات PQ التي تم تحديدها. يستخدم برنامج Matlab Simulink لمحاكاة شبكة الطاقة ، والأحمال ، ومغز الجهد الديناميكي (DVR). يتم استخدام (JFS) للحصول على قيم الكسب لوحدة التحكم PI لجهاز DVR المقترح. تؤيد نتائج Matlab / Simulink فعالية الجهاز المقترح وقوته وزمن وصوله.

الكلمات المفتاحية : مشكلات جودة القدرة , انخفاض الجهد الكهربى , عدم اتزان الجهد الكهربى , مسترجع الجهد الديناميكي

1. INTRODUCTION

Electrical power should always be available because it is a necessary requirement of all commercial and industrial operations. Power quality is a set of parameters that define the characteristics of the power supply as delivered to consumers under normal operating conditions in terms of supply continuity and voltage characteristics such as frequency, magnitude, waveform, and symmetry. Recently, power quality has become not only a technical issue but also a financial issue [1]. The power system is organized in three sections: generation, transmission and distribution. The power could be fed to various loads on the distribution side via other transmission lines. Power quality in the power system becomes crucial when fluctuating power is provided to the load [2].

For the following reasons, power quality is becoming more important: Power electronic devices and advanced equipment with microprocessor-based controls are more sensitive to variations in power quality, and the use of power electronic devices for control of variable speed drives and switched mode is perceived, especially by the service sectors, such as hospitals, as causing a lot of electrical disturbances in the supply system [3].

Power quality issues include a wide range of disturbances such as voltage sags, unbalance, swells, flickers, harmonic distortion, impulse transients, and interruptions, at their installations, industrial, commercial, and residential customers use a large number of power electronics devices; these devices are sensitive to power quality disturbances.

According to studies and surveys conducted in various countries around the world, industries are susceptible to reliability issues (long and short interruptions). Voltage sag is the most serious power quality problem in the manufacturing and telecommunications industries [1]. Author investigates the impact of power quality issues on power systems and load in Ref [4]. The current capacity of different electrical components, including cables, transformers, and transmission lines, was also suggested in that paper to be significantly influenced by harmonics. Al-Badri discovered that non-linear loads, such as those created by power electronics devices in use, arc furnaces, and the resonance of shunt capacitor and/or inductor series, produce harmonics in the power system. [5]. Several mitigation techniques, such as distribution line reconfiguration, phase rearrangement, and phase balancing between particular medium voltage feeders and the power distribution energy converter banks with a radial arrangement system, have been proposed in the past by various researchers to reduce voltage variation and improve the voltage profile in distribution systems. [6], [7]. The consequence of voltage imbalance on the procedure of induction motors is investigated in Refs [8], [9]. Gnacinski and colleague [10]. Voltage imbalance was uncovered to heat the windings faster than other power quality problems. The standards of power quality and their applications are summarised in Ref [11]. According to a study published in [12], unbalanced voltage supply and harmonics may coexist in the grid when their causes do (for example, an induction motor with phase asymmetry or in an imbalanced power network, driven by variable-frequency drives), according to a study by Sousa et al. Martiningsih et al. instructed installing a DVR in the Pay TV Dian Swastatika Sentosa services (PT DSS) power plant; the DVR operates as a compensator and is connected in series with the distribution line. The proposed PI-based DVR is capable of resolving power quality constraints [13]. Eltamaly et al. created a DVR-based technique for voltage sag mitigation and power system quality improvement. The performance of electrical equipment has declined. The findings show that DVR adequately compensates for sag/swell and implements appropriate

voltage adjustment [14]. In order to reduce symmetrical and asymmetrical sags, a unique DVR with a power electronic transformer was presented. Results demonstrate that symmetrical and asymmetrical voltage sag on distribution lines is successfully reduced by the modern design [15]

This paper investigates voltage sag and voltage unbalance, which are applied on real nonlinear loads consisting of two large induction motors, and the DVR is proposed as a solution to these issues.

The main contribution of this article can be summarized as follows:

1. The real distribution system located at Beshai Company in Sadat city, Egypt is presented.
2. Build up the DVR scheme and its application in the presented model.
3. A proposal for gorilla troops optimization algorithm in order to get the PI controller's gain values in DVR topology.
4. Two power quality issues of voltage sag and unbalanced conditions are presented.

2. POWER QUALITY PROBLEMS CLASSIFICATION

There is always a relation between the voltage and the current, and power quality is a combination of voltage and current quality. Voltage quality in any practical power system is generally the utility's responsibility [16].

2.1. Voltage Sag

Voltage sag, characterized by IEEE averages 1159-1995 as a decrease in the value of the voltage between 0.1 and 0.9 pu at the power commonness with a period of 0.5 cycles to 1 minute, is one of the most important causes of poor power quality [17].

2.1.1. The causes of voltage sag

The causes of voltage sag can be summarized as follows: -

- Voltage sag caused by faults is mostly caused by power system faults. The type of fault and the distance between the source and the fault determines the severity of sag. A three-phase fault near a distribution substation causes deep sag in all customers connected to that substation [3], [17]. Weather (snow, wind, and lightning) and interference from smaller animals and birds are the most common causes of power system failures.
- Operation of circuit breaker: The operation of a circuit breaker causes a temporary fault on a specific line. Because of this temporary fault, voltage sags in neighboring lines will occur in the event of a weak grid. The extent of the voltage sag is determined by the distance between the supply voltage and the fault.
- Energizing the transformer: Many transformers are used in the medium voltage line. When this line is operational, both transformers energize at the same time, resulting in a very high current flow. This causes short duration voltage drop. This is known as voltage sag, and its effect is visible to consumers.
- Starting of Induction Motor: Induction motors require a high starting current that is five to six times the nominal value of the motor. This high current persists until the induction motor begins to run at the nominal speed. The voltage drop is determined by the power system and induction motor specifications [18].

2.2. Voltage Unbalance (Imbalance)

According to IEEE, voltage unbalance is defined as the negative or zero sequence component divided by the positive sequence component. It is a voltage variation in a power system in which the magnitudes of the voltages or the phase angle differences between them are not equal [19]. As a result, only polyphase systems are affected by this power quality issue (e.g., three-phase).

The percent Voltage Unbalance Factor (VUF) is defined by European standards as the ratio of the negative sequence voltage to the positive sequence voltage [20]. The voltage unbalance factor should be less than "2 to 3 " according to IEEE Std. 1547.2 – 2008.

3. SYSTEM CONFIGURATION

The system under study comprises large induction motors, each has 6.7 MW, which is fed from a busbar with 11 kV, where it is outgoing from step-down transformer with 220/11 kV, located at Beshai Company in Sadat city, Egypt. The power is transmitted from the transformer to the load through a 0.8 km underground cable, as shown in Fig. 1. Table 1 lists the electrical equipment's parameters.

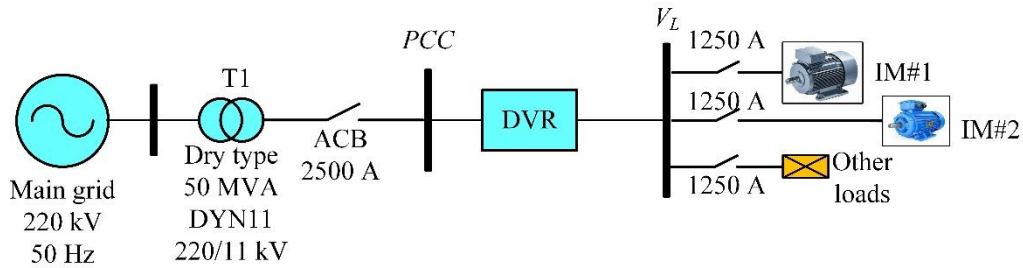


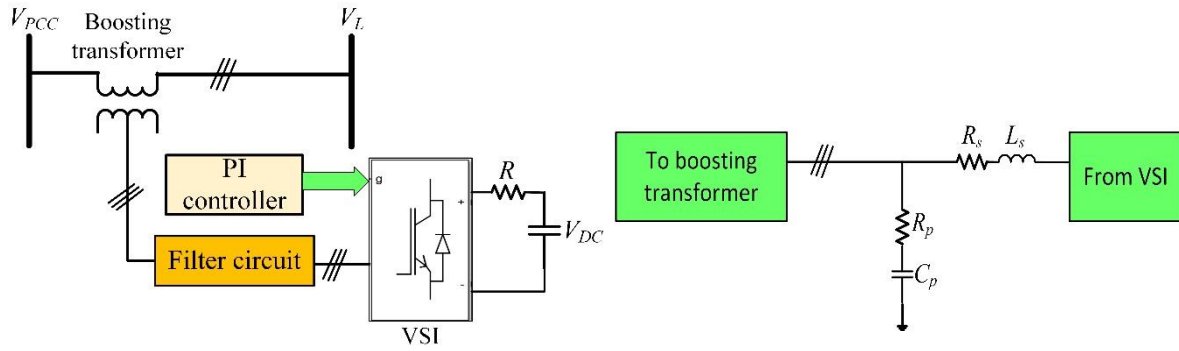
Fig. 1: Single-line diagram for a system under study.

Table 1: The electrical equipment's parameters.

Elements	Parameters
Utility	50 MVA, 220 kV, 50 Hz
Transformer	DYN11, 220/11kV, 50 MVA
TL	L=0.8 km, R=0.113 Ω/km, L=0.18 mH/km
Two induction motors (IM)	P=6700 kW, I=398 A, n=1394 rpm, V=11 kV, PF=0.91
Others loads (nonlinear load)	P=500 W, Qc=500 var, V=11 kV
DVR rating	750 KVA

4. DYNAMIC VOLTAGE RESTORER

It is proposed that a dynamic voltage restorer be used to mitigate the mentioned power quality issues. The presented DVR structure is installed between the V_g and V_L buses and functions as a PQ conditioner to improve voltage, compensate for reactive power, and reduce harmonic distortion. The proposed DVR, depicted in Fig. 3, is made up of a series of a capacitor connected on the AC side of three single-phase boosting transformers. To control the flow of power, a series resistance is connected in series with a capacitor bank [21]. Table 2. shows the detailed parameters of the DVR scheme.



a) Scheme diagram of DVR b) Circuit design of the filter
Fig. 3: Functional model of the DVR scheme.

Table 2: The detailed specification of the DVR scheme.

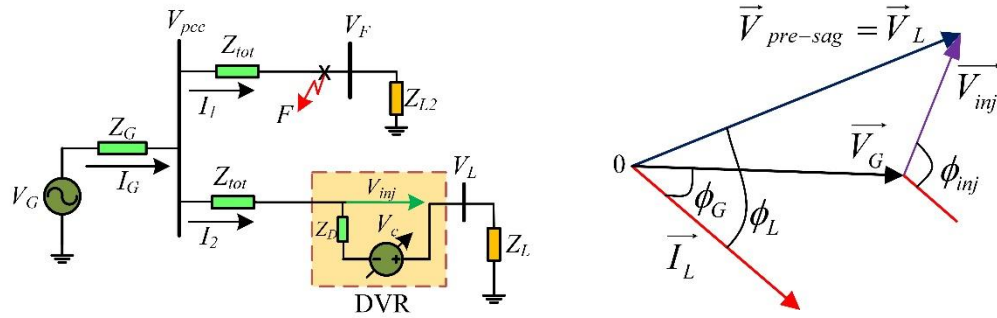
Part	Value	Part	Value
V_{DC}	7000V	Filter shunt resistance (R_p)	60 Ω
R	0.1 Ω	Filter shunt capacitance (C_p)	6 μ F
f	50 Hz	Filter series inductance (L_s)	80 mH
Voltage source inverter	3 arms, 6 pulses	Filter series resistance (R_s)	0.1 Ω
Carrier frequency	5000 Hz	Boosting transformer ratio	1:1

The proposed DVR, depicted in **Fig. 3**, consists of the following components:

- a) **Energy Storage (ES)** : Its primary function is to provide the desired real power to the DVR during compensation. It can be represented as a battery, or super capacitors can be used as a fast-responding storage element [22, 23].
- b) **Voltage source inverter (VSI)** : It is used to convert voltage from the DC battery to AC to inject the desired voltage magnitude, phase, and frequency into the transformer [24].
- c) **Boosting transformer** : It transfers the voltage required for compensation from the universal bridge to the distribution network. The primary winding is linked to the power system in series, while the secondary winding is linked to the universal bridge unit.
- d) **Filter circuit** : It includes an RLC circuit to reduce harmonic distortion in the VSI-generated waveform.
- e) **PI Controller** : It represents the supervisor in charge of controlling the load voltage. In other words, it compares the load bus signal voltage to the reference voltage to drive the PI Controller [25].

4.1. Operating principle of the proposed DVR

Fig. 4 (a) depicts a Thevenin circuit of the system under consideration, with its comparable voltage source V_G and source impedance Z_G preselected [29]. It provides two packs denoted by their impedances Z_L and Z_{L2} via two feeder V_F and V_L , where Z_{tot} denotes the feeder impedance. During normal operation, the common bus pre-sag voltage ($V_{Pre-sag}$) and line current (I_G) are calculated using Kirchoff's voltage law (KVL) for a typical DVR, as shown in Eqs. (1) and (2):



a) Thevenin equivalent circuit of DVR scheme

b) Phasor diagram for DVR

Fig. 4: Principle of operation.

$$V_{pre-sag} = V_G - I_G Z_G \quad (1)$$

$$I_S = I_1 + I_2 = \frac{V_{pre-sag}}{Z_{tot} + Z_{L2}} + \frac{V_{pre-sag}}{Z_{tot} + Z_{L1}} \quad (2)$$

When a fault (F) occurs on the feeder, the highest current (I_{Sfault}) flows through it. The voltage at the PCC during sag (V_{sag}), will give by the Eqs (3) and (4).

$$V_{sag} = V_G - I_{Sfault} Z_S \quad (3)$$

$$I_{Sfault} = I_1 + I_2 = \frac{V_{sag}}{Z_{tot}} + \frac{V_{sag}}{Z_{tot} + Z_{L1}} \quad (4)$$

As a result, the phasor diagram is shown in Figure 4. (b) Depicts the injected voltage (V_{inj}) during the sag condition. Eqs. (5) and (6) Determine the magnitude and angle of the injected voltage:

$$|V_{inj}| = \sqrt{V_L^2 + V_G^2 - 2V_L V_G \cos(\phi_L - \phi_G)} \quad (5)$$

$$\phi_{inj} = \tan^{-1} \left(\frac{V_L \sin \phi_L - V_G \sin \phi_G}{V_L \cos \phi_L - V_G \cos \phi_G} \right) \quad (6)$$

The three-phase reference voltage is summed as follows:

$$\begin{bmatrix} V_{Aref} \\ V_{Bref} \\ V_{Cref} \end{bmatrix} = V_{L-max} \begin{bmatrix} \sin \omega t \\ \sin \left(\omega t - \frac{2\pi}{3} \right) \\ \sin \left(\omega t + \frac{2\pi}{3} \right) \end{bmatrix} \quad (7)$$

Then, using the Park transformation, it is transformed from three-phase abc-to-dq0 components as follows:

$$\begin{bmatrix} V_d \\ V_q \\ V_0 \end{bmatrix} = \frac{2}{3} \begin{bmatrix} \cos(\omega t) & \cos(\omega t - \frac{2\pi}{3}) & \cos(\omega t + \frac{2\pi}{3}) \\ -\sin(\omega t) & -\sin(\omega t - \frac{2\pi}{3}) & -\sin(\omega t + \frac{2\pi}{3}) \\ \frac{1}{2} & \frac{1}{2} & \frac{1}{2} \end{bmatrix} \begin{bmatrix} V_a \\ V_b \\ V_c \end{bmatrix} \quad (8)$$

4.2. The Proposed Control Scheme for DVR

Voltage disturbances that occur in the system are detected. As shown in **Fig. 4**, V_L is compared to a reference voltage. The controller is timed to the supply voltage.

The controller scheme is presented. The gate pulses are generated as an output of the DVR voltages to drive the VSI, which absorbs increasing voltage and compensates for decreasing voltage which absorbs increasing voltage and compensates for decreasing voltage [27]. The proposed DVR can be controlled in five steps, as shown below [26].

First: the kind of voltage disturbance is essential for deciding the span time (start and end points), depth, and stage jump [28]. represents various approaches load voltages $V_{L, abc}$, and reference voltages $V_{ref, abc}$ are vectorized dq0 voltage elements $V_{L, dq0}$, and the primary goal of series compensation should be emphasized: to suppress a portion of the feeders' line reactance to improve load voltage. $V_{ref, dq0}$ in this study using the Park transformation.

Second: The error signal defined as a voltage magnitude and phase shift will be obtained after transforming the load voltage and reference voltage to the dq0 frame.

$$|e_{t,dq0}| = \sqrt{(V_{ref,d} - V_{L,d})^2 + (V_{ref,q} - V_{L,q})^2 + (V_{ref,0} - V_{L,0})^2} \quad (9)$$

Any magnitude and phase shift in the voltage will cause a change in the dq0 components. The new control detects changes in the state of the supply and responds quickly.

Third: Synchronization to the supply voltage, as introduced in [29], is an important step for adequate control of the presented DVR. It keeps the controller's output signal synchronised with a reference input signal in frequency and phase. As a result, a phase-locked loop (PLL) is used as a synchronisation tool in this work.

Fourth: The presented DVR control has a low complexity because it is based on an error-driven PI controller. The controller's function is to adjust the error signal so that it is minimised on the distribution grid, as shown in **Fig. 5**. Furthermore, in the time domain, V_c represents the contribution signal in the dq0 frame of the DVR's PWM for the PI controller, as shown below:

$$V_{c,dq0} = K_p e_{t,dq0} + K_i \int_0^1 e_{t,dq0} dt \quad (10)$$

Fifth: Finally, the PI controller output returns to the three-phase abc frame to control the PWM for generating the gating pulses to drive the VSI, as shown below:

$$\begin{bmatrix} V_{c1.a} \\ V_{c1.b} \\ V_{c1.c} \end{bmatrix} = \begin{bmatrix} \sin(\omega t) & \cos(\omega t) & 1 \\ \sin(\omega t - \frac{2\pi}{3}) & \cos(\omega t - \frac{2\pi}{3}) & 1 \\ \sin(\omega t + \frac{2\pi}{3}) & \cos(\omega t + \frac{2\pi}{3}) & 1 \end{bmatrix} \begin{bmatrix} V_{c1.d} \\ V_{c1.q} \\ V_{c1.0} \end{bmatrix} \quad (11)$$

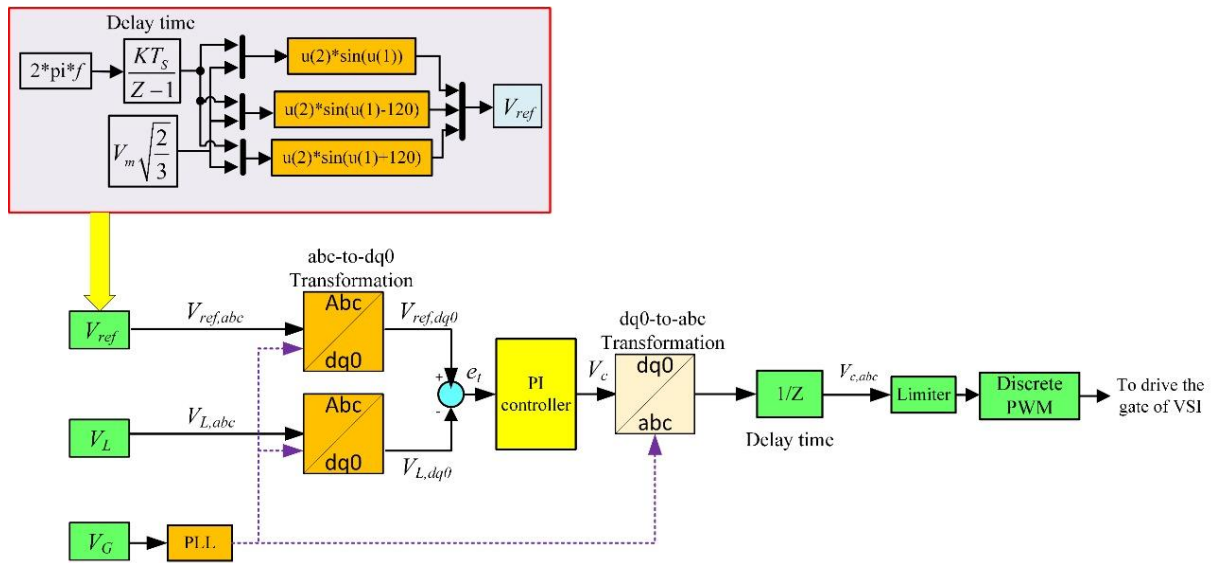


Fig. 5. Scheme of proposed control strategy.

5. OPTIMIZATION OF THE OPTIMIZATION PROBLEM

5.1. Fitness function

The fitness function is used to adjust the gains of the proposed DVR-PI controllers and is defined as:

$$\min(J) = \min(ITAE) = \int_0^{\infty} t|e_t| dt \quad (12)$$

Where J is the proposed DVR controller's overall error, and ITAE stands for integral time absolute error. e_t represents the error signal. The optimization problem is subject to the following constraints.

5.2. Constraints

The second feeder's voltage level is restricted to the range between its minimum and maximum values, as determined by Eq (13), thus

$$0.95 \leq V_L \leq 1.05 \quad (13)$$

5.3. Jellyfish Search Optimization Technique

The Jellyfish search (JFS) optimization algorithm is a novel optimization method that is mesmerized by the motion of jellyfish. Three categories have been established for them. The jellyfish could first flow in the direction of the ocean current or within its own swarm. In the meantime, whenever, the jellyfish are drawn to areas where there is an adequate supply of food. The numerical fitness function also shows the amount of food consumed [30], [31]. The initial population could be expressed mathematically as follows [32]:

$$X_i(t+1) = 4P_0(1 - X_i). \quad 0 \leq P_0 \leq 1 \quad (14)$$

$X_i(t + 1)$ denotes the jellyfish chaotic counterpart. where $P0$ is a randomly chosen number between $[0, 1]$ and does not equal $[0.0, 0.25, 0.75, 0.5, 1.0]$. and Equation (15) describes how the time control function's value evaluated (CF), which changes from 0 to 1 [33].

$$CF(t) = \left| \left(1 - \frac{t}{T^{max}} \right) \times (2 \times r_1 - 1) \right| \quad (15)$$

where t denotes the iteration count; T^{max} specifies the maximum number of iterations, while r_1 is a randomly generated value between $[0, 1]$. Equation (16) [32] illustrates how to develop the fresh location of each jellyfish if the CF value is more than 0.5

$$X_i(t + 1) = R \times (X^* - 3 \times R \times \mu) + X_i(t) \quad (16)$$

where μ represents the jellyfish population's average, X^* represents the jellyfishes' best placement within the population, and R is an integer drawn at random from the range $[0, 1]$. Based on the minimum fitness value, the best position among the jellyfish in the population is determined. The fitness function, which is defined as the volume of food, is assessed over the entire population of jellyfish. The first one is selected as having the best position after they are sorted in ascending order. According to the movement inside the swarm, the fresh location of each jellyfish may be determined if the CF value is less than 0.5, using either Equation (17) to represent the passive type or Equation (17) to follow the active type, as illustrated in [32].

$$X_i(t + 1) = 0.1 \times R \times (U_b - L_b)X_i(t) \quad (17)$$

$$X_i(t + 1) = \begin{cases} X_i(t) + R(X_j(t) - X_i(t)) & \text{if } f(X_i) \geq f(X_j) \\ X_i(t) + R(X_j(t) - X_i(t)) & \text{if } f(X_i) < f(X_j) \end{cases} \quad (18)$$

where U_b and L_b stand for the control parameters' upper and lower bounds, respectively, and f represents the amount of food in each jellyfish location's qualitative function. The upper and lower bounds of the control parameters are related to the open links for reconfiguration. The checking model for each jellyfish position to be restored at the closest border is also described in Equation (19).

$$\begin{cases} X'_{i,d} = (X_{i,d} - U_{b,d}) + L_b(d) & \text{if } X_{i,d} > U_{b,d} \\ X'_{i,d} = (X_{i,d} - L_{b,d}) + U_b(d) & \text{if } X_{i,d} < L_{b,d} \end{cases} \quad (19)$$

where $X'_{i,d}$ denotes the position of the i th jellyfish in the d th dimension. The number of control parameters, which are defined as the open linkages for reconfiguration as in Equation (20), is the dimension for the jellyfish place. The main phases of the JFS are shown in **Fig. 6**.

$$VI = \{ \underbrace{[O_{T1} O_{T1} \dots \dots O_{TON}]} \} \quad (20)$$

Open tie branch

the vector of the variables independent (VI) looks like this where, O_T is the tie lines to be open and No is their number. The open tie links must always be assigned an integer value that is limited by the total number of DN lines, as shown in equation (21).

$$1 \leq O_{Tj} \leq No \quad j = 1.2 \dots \dots \dots No \quad (21)$$

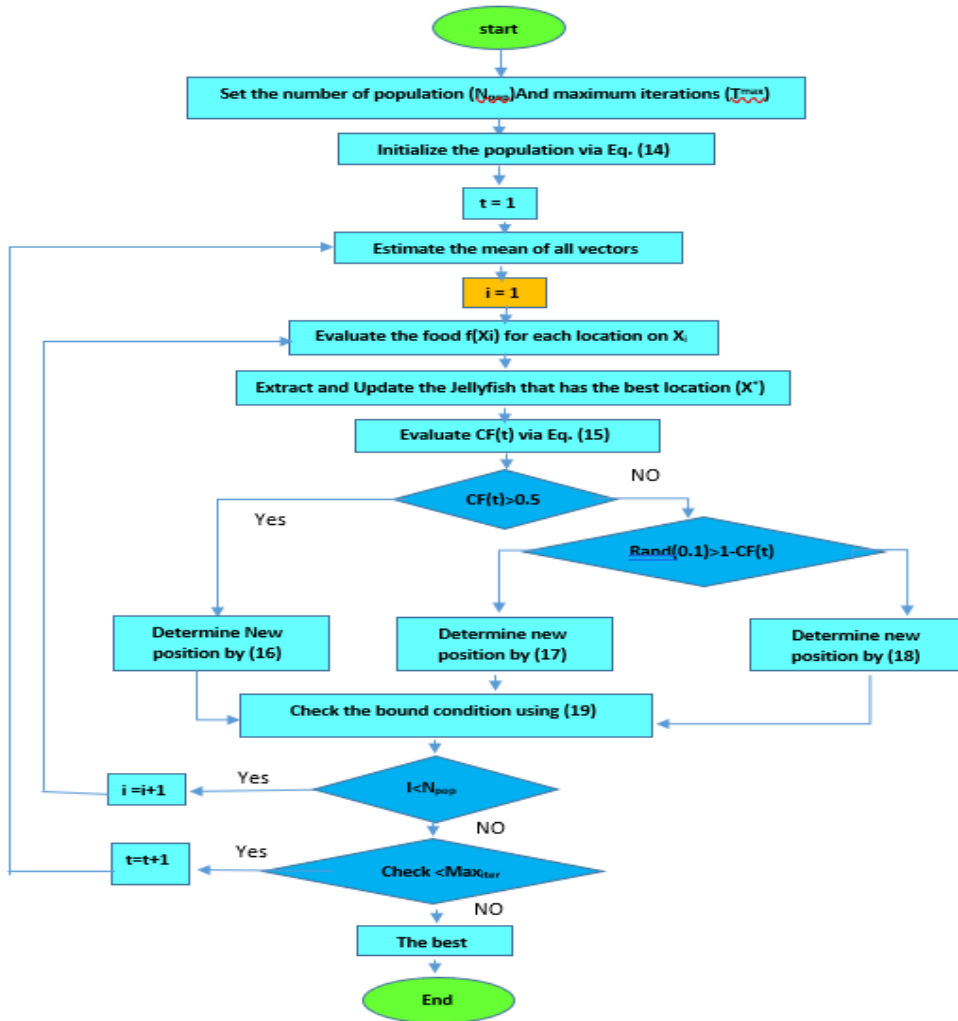


Fig. 6: Main phases of the JFS.

6. DIGITAL SIMULATION RESULTS

As illustrated in **Fig.7,8**, the newly introduced DVR is tested using the MATLAB/Simulink platform, demonstrating enhancing voltage sag and unbalanced conditions.

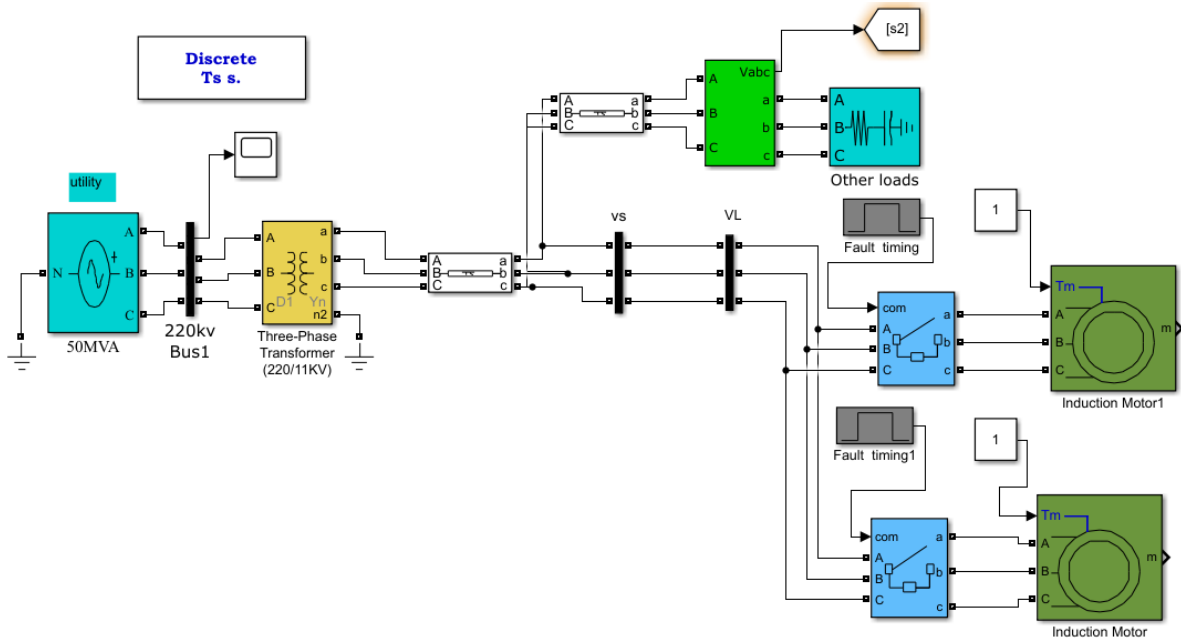


Fig .7: MATLAB Simulink of the system under study with load.

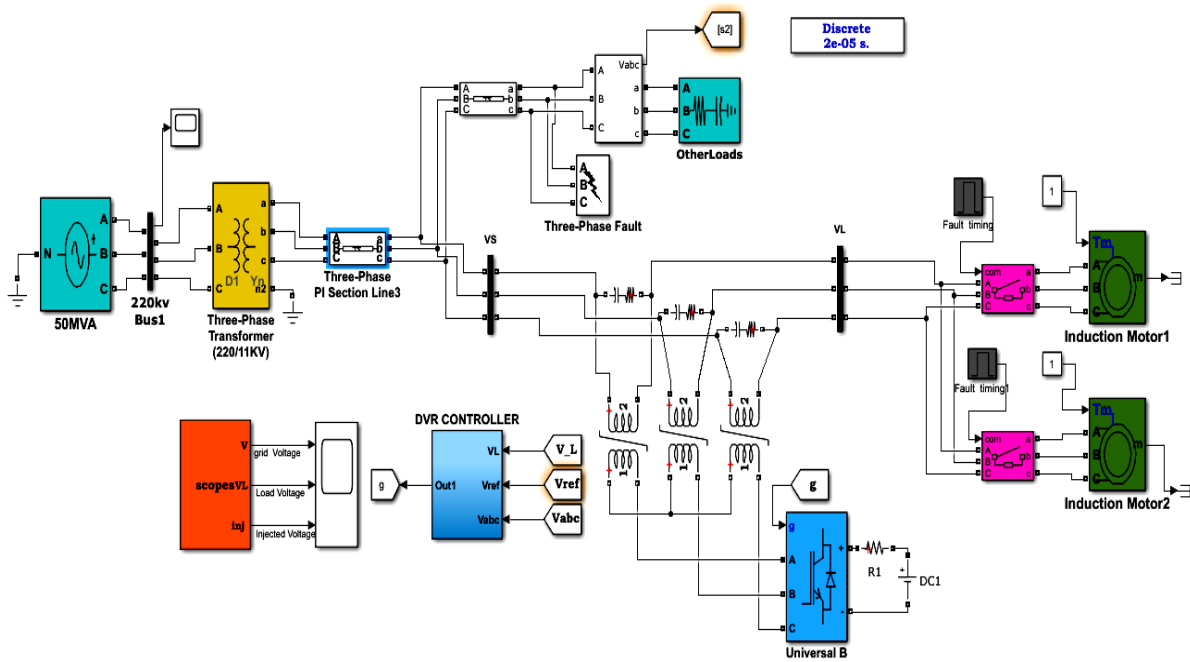


Fig .8: MATLAB Simulink of the system under study after connecting DVR.

6.1. Voltage Sag Condition

At the time intervals $t = 0.1$ s and $t = 0.2$ s, a three-phase induction motor is started. As a result, a balanced voltage sag mode develops. When the DVR is shown during this event. The DVR injects the necessary voltage into the three phases and then improves the load voltage profile of the system under study, as shown in **Fig.9**.

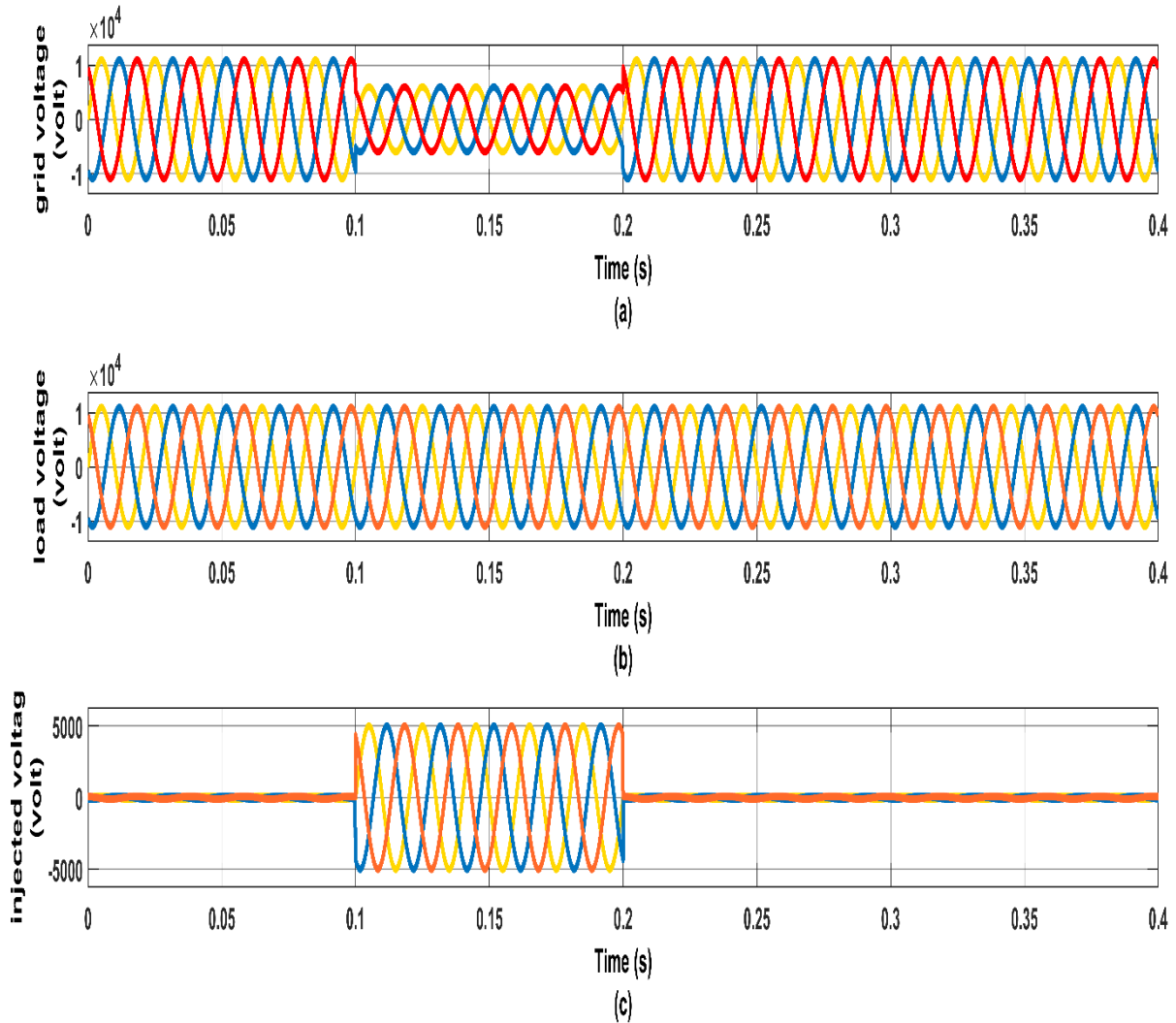


Fig. 9: Results for sag condition

a) Grid voltage in volts, b) Compensated load voltage in volts and c) Injected voltage in volts.

6.2. Voltage Unbalance Condition

An unbalance condition occurs at the first feeder between $t=0.1$ s and $t=0.3$ s. During this event condition, the DVR rapidly injects the required voltage. The voltage profile at V_L before and after compensation, as well as the injected voltage are shown in **Fig.10**.

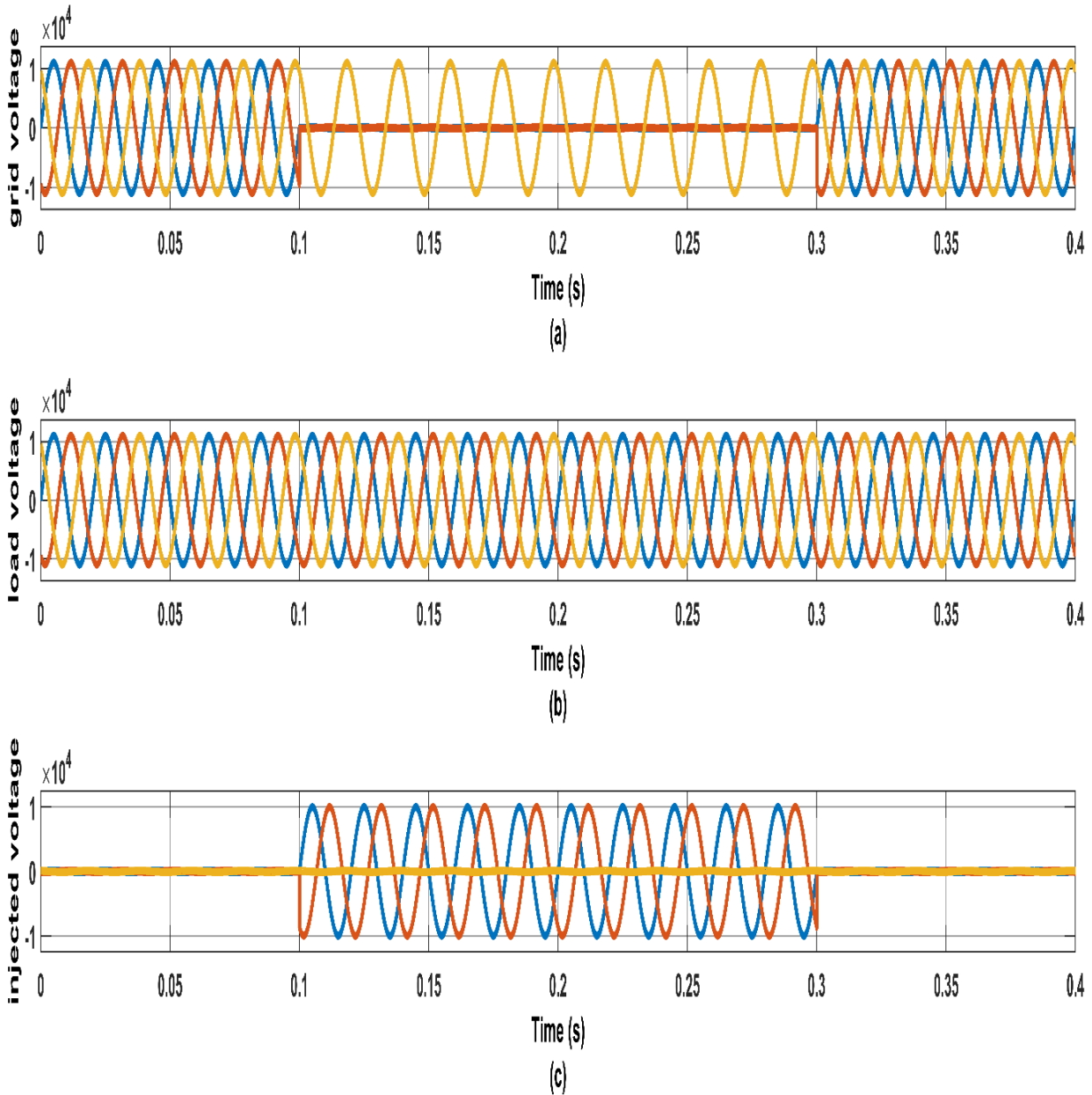


Fig. 10: Results for unbalance condition

a) Grid voltage in volts, b) Compensated load voltage in volts and c) Injected voltage in volts.

7. CONCLUSIONS

Voltage sag and voltage unbalance were presented as two different power quality issues in this work. Each of these power quality problems was investigated using a large load. Beshai-considered Company's load is high power induction motors. It has been discovered that starting high power induction motors causes a voltage sag at the point of common coupling (PCC). Voltage unbalance was also caused by a double line to ground fault. As a series compensation device, the dynamic voltage restorer (DVR) scheme is used. To address power quality issues associated with industrial loads connected to a distribution network, (DVR) is proposed to improve voltage sag and voltage unbalance. The jellyfish search optimizer (JFS) is utilized to get the gain values of the PI controller for the proposed DVR. The results advocate the proposed device's effectiveness, robustness, and latency.

REFERENCES

- [1] Ali, A. J. F., Zayer, W. H., & Shukir, S. S. (2019). Power quality problems and improvement techniques. *J. Eng. Appl. Sci*, 14, 5888-5898.
- [2] Abas, N., Dilshad, S., Khalid, A., Saleem, M. S., & Khan, N. (2020). Power quality improvement using dynamic voltage restorer. *IEEE Access*, 8, 164325-164339.
- [3] Mohammed, A. B., Ariff, M. A. M., & Ramli, S. N. (2020). Power quality improvement using dynamic voltage restorer in electrical distribution system: an overview. *Indonesian Journal of Electrical Engineering and Computer Science (IJEECS)*, 17(1), 86-93.
- [4] Jassim, A. H., Hussein, A. A., & Abbas, L. F. (2021, February). Study the performance of three-phase induction motor under imbalanced non-sinusoidal supply. In *IOP Conference Series: Materials Science and Engineering* (Vol. 1058, No. 1, p. 012035). IOP Publishing.
- [5] Al-Badri, M., Pillay, P., & Angers, P. (2017). A novel in situ efficiency estimation algorithm for three-phase induction motors operating with distorted unbalanced voltages. *IEEE Transactions on Industry Applications*, 53(6), 5338-5347.
- [6] Ogunboyo, P. T., Tiako, R., & Davidson, I. E. (2018). Effectiveness of dynamic voltage restorer for unbalance voltage mitigation and voltage profile improvement in secondary distribution system. *Canadian Journal of Electrical and Computer Engineering*, 41(2), 105-115.
- [7] Soomro, A. H., Larik, A. S., Mahar, M. A., Sahito, A. A., Soomro, A. M., & Kaloi, G. S. (2021). Dynamic voltage restorer—A comprehensive review. *Energy Reports*, 7, 6786-6805.
- [8] Ferreira, F. J., & Sousa Santos, V. (2018). Unbalanced voltages impacts on the energy performance of induction motors.
- [9] Adouni, A., & J. Marques Cardoso, A. (2020). Thermal analysis of low-power three-phase induction motors operating under voltage unbalance and inter-turn short circuit faults. *Machines*, 9(1), 2.
- [10] Gnaciński, P., Pepliński, M., Hallmann, D., & Jankowski, P. (2019). Induction cage machine thermal transients under lowered voltage quality. *IET Electric Power Applications*, 13(4), 479-486.
- [11] Boldea, I., & Nasar, S. A. (2018). *The induction machines design handbook*. CRC press.
- [12] Santos, V. S., Eras, J. J. C., Gutiérrez, A. S., & Ulloa, M. J. C. (2019). Assessment of the energy efficiency estimation methods on induction motors considering real-time monitoring. *Measurement*, 136, 237-247.
- [13] Martiningsih, W., & Prakoso, U. Y. (2018). Power quality improvement using dynamic voltage restorer in distribution system PT. DSS Power Plant. In *MATEC Web of Conferences* (Vol. 218, p. 01003). EDP Sciences.
- [14] Eltamaly, A. M., Sayed, Y., El-Sayed, A. H. M., & Elghaffar, A. N. A. (2018). Mitigation voltage sag using DVR with power distribution networks for enhancing the power system quality. *IJEEAS Journal*, 1(2).
- [15] Ali, K. K., Talei, M., Siadatan, A., & Rad, S. M. H. (2017, October). Power quality improvement using novel dynamic voltage restorer based on power electronic transformer. In *2017 IEEE Electrical Power and Energy Conference (EPEC)* (pp. 1-6). IEEE.

- [16] Hasan, S., Muttaqi, K. M., Sutanto, D., & Bouzardoum, A. (2020). Calculation of the Voltage Sag Recovery Point-on-Wave and Sag Duration Using System Parameters. *IEEE Transactions on Industry Applications*, 56(4), 4588-4601.
- [17] Mishra, M. (2019). Power quality disturbance detection and classification using signal processing and soft computing techniques: A comprehensive review. *International transactions on electrical energy systems*, 29(8), e12008
- [18] Babu, V., Ahmed, K. S., Shuaib, Y. M., & Manikandan, M. (2021). Power Quality Enhancement Using Dynamic Voltage Restorer (DVR)-Based Predictive Space Vector Transformation (PSVT) With Proportional Resonant (PR)-Controller. *IEEE Access*, 9, 155380-155392.
- [19] Igual, R., & Medrano, C. (2020). Research challenges in real-time classification of power quality disturbances applicable to microgrids: A systematic review. *Renewable and Sustainable Energy Reviews*, 132, 110050.
- [20] Electrical Power & Energy Conference (EPEC), 2009 IEEE : date, 22-23 Oct. 2009. IEEE, 2009.
- [21] Farhadi-Kangarlu, M., Babaei, E., & Blaabjerg, F. (2017). A comprehensive review of dynamic voltage restorers. *International Journal of Electrical Power & Energy Systems*, 92, 136-155.
- [22] Zobaa, A. F., Ribeiro, P. F., Aleem, S. H. A., & Afifi, S. N. (Eds.). (2018). Energy storage at different voltage levels: technology, integration, and market aspects (Vol. 111). *Energy Engineering*.
- [23] Omar, A. I., Sharaf, A. M., Abdel, A. S. H., Mohamed, A. A., & EA, E. Z. E. (2019, December). Optimal Switched Compensator for Vehicle-To-Grid Battery Chargers Using Salp Optimization. In *2019 21st International Middle East Power Systems Conference (MEPCON)* (pp. 139-144). IEEE.
- [24] H. F. Sindi, S. Alghamdi, M. Rawa, A. I. Omar, and A. Hussain Elmetwaly, (2022, "Nov.). Robust control of adaptive power quality compensator in Multi-Microgrids for power quality enhancement using puzzle optimization algorithm,"
- [25] Awad, M., Ibrahim, A. M., Alaas, Z. M., El-Shahat, A., & Omar, A. I. (2022). Design and analysis of an efficient photovoltaic energy-powered electric vehicle charging station using perturb and observe MPPT algorithm. *Front. Energy Res*, (10), 969482. *Ain Shams Engineering Journal*, p. 102047, doi: 10.1016/j.asej.2022.102047.
- [26] Omar, A. I., Aleem, S. H. A., El-Zahab, E. E., Algablawy, M., & Ali, Z. M. (2019). An improved approach for robust control of dynamic voltage restorer and power quality enhancement using grasshopper optimization algorithm. *ISA transactions*, 95, 110-129.
- [27] Elmetwaly, A. H., ElDesouky, A. A., Omar, A. I., & Saad, M. A. (2022). Operation control, energy management, and power quality enhancement for a cluster of isolated microgrids. *Ain Shams Engineering Journal*, 13(5), 101737.
- [28] Afonso, J. L., Tanta, M., Pinto, J. G. O., Monteiro, L. F., Machado, L., Sousa, T. J., & Monteiro, V. (2021). A Review on Power Electronics Technologies for Power Quality Improvement. *Energies*, 14(24), 8585.
- [29] Ezzeldin, R., El-Ghandour, H., & El-Aabd, S. (2022). Optimal management of coastal aquifers using artificial jellyfish search algorithm. *Journal of Hydrology : Regional Studies*, 41, 101058
- [30] Ragab, E. L., Shaheen, A., Ginidi, A., Ghoneim, S., Alharthi, M., & Elsayed, A. (2022). Quasi-reflection jellyfish optimizer for optimal power flow in electrical power systems. *Studies in Informatics and Control*, 31(1), 49-58.
- [31] Chou, J. S., & Truong, D. N. (2021). A novel metaheuristic optimizer inspired by behavior of jellyfish in ocean. *Applied Mathematics and Computation*, 389, 125535.
- [32] Abdel-Basset, M., Mohamed, R., Chakraborty, R. K., Ryan, M. J., & El-Fergany, A. (2021). An improved artificial jellyfish search optimizer for parameter identification of photovoltaic models. *Energies*, 14(7), 1867